

Programmed elimination of cells by caspase-independent cell extrusion in *C. elegans*

Daniel P. Denning¹, Victoria Hatch¹ & H. Robert Horvitz¹

The elimination of unnecessary or defective cells from metazoans occurs during normal development and tissue homeostasis, as well as in response to infection or cellular damage¹. Although many cells are removed through caspase-mediated apoptosis followed by phagocytosis by engulfing cells², other mechanisms of cell elimination occur³, including the extrusion of cells from epithelia through a poorly understood, possibly caspase-independent, process⁴. Here we identify a mechanism of cell extrusion that is caspase independent and that can eliminate a subset of the *Caenorhabditis elegans* cells programmed to die during embryonic development. In wild-type animals, these cells die soon after their generation through caspase-mediated apoptosis. However, in mutants lacking all four *C. elegans* caspase genes, these cells are eliminated by being extruded from the developing embryo into the extra-embryonic space of the egg. The shed cells show apoptosis-like cytological and morphological characteristics, indicating that apoptosis can occur in the absence of caspases in *C. elegans*. We describe a kinase pathway required for cell extrusion involving PAR-4, STRD-1 and MOP-25.1/25.2, the *C. elegans* homologues of the mammalian tumour-suppressor kinase LKB1 and its binding partners STRAD α and MO25 α . The AMPK-related kinase PIG-1, a possible target of the PAR-4-STRD-1-MOP-25 kinase complex, is also required for cell shedding. PIG-1 promotes shed-cell detachment by preventing the cell-surface expression of cell-adhesion molecules. Our findings reveal a mechanism for apoptotic cell elimination that is fundamentally distinct from that of canonical programmed cell death.

The caspase CED-3 is essential for nearly all programmed cell deaths that occur during *C. elegans* development⁵. However, a few cells undergo programmed cell death in *ced-3* mutants⁵⁻⁷. We observed that some cells are eliminated from *ced-3*-mutant embryos by being shed from the developing animal. The eggs of *ced-3* mutants but not those of wild-type animals contained on average six shed cells that had detached during the comma stage of embryogenesis (~300 min after fertilization) (Fig. 1a-c, f and Supplementary Table 1). The shed cells detached at the anterior sensory depression or the ventral pocket (Fig. 2a, b) and remained within the egg (but separate from the animal) throughout embryogenesis. Embryos with a loss-of-function mutation in the *APAF1* homologue *ced-4* or the BH3-domain-encoding gene *egl-1*, or a gain-of-function mutation of the *BCL2* homologue *ced-9* also produced shed cells (Fig. 1c), indicating that a defect in any step of the execution phase of programmed cell death can generate shed cells. As reported previously⁸, mutant embryos defective in engulfment (for example, *ced-1*- or *ced-5*-mutant embryos) contain 'floaters' (Fig. 1c, d, g and Supplementary Table 1), cells that undergo CED-3-mediated apoptosis and detach from the embryo because they cannot be internalized by engulfing cells. In comparison to *ced-3*-mutant shed cells, *ced-5*-mutant floaters were smaller, more uniformly refractile when viewed by Nomarski optics, and less likely to aggregate into clumps of three or more cells after detachment (Fig. 1a, b, d and Supplementary Table 1). *ced-3* mutations were epistatic to engulfment mutations with respect to the number of shed cells, their appearance

and their tendency to aggregate (Supplementary Table 1; data not shown). Thus, the shed cells of embryos defective in programmed cell death are genetically and morphologically distinguishable from those of embryos defective in engulfment.

The *C. elegans* genome encodes three additional caspase homologues: *csp-1*, *csp-2* and *csp-3* (ref. 9). We determined that individual *csp* mutations did not cause the appearance of shed cells (Supplementary Fig. 1 and Supplementary Table 2). Eggs from quadruple mutants lacking all four caspase genes (*csp-1*, *csp-2*, *csp-3* and *ced-3*), like *ced-3*-mutant eggs, contained on average six shed cells (Fig. 1c, e), indicating that the generation of shed cells is caspase independent.

Although caspase activation can drive apoptosis, recent studies have suggested that caspases are not necessary for apoptosis³. We therefore examined *csp-3*; *csp-1*; *csp-2* *ced-3* quadruple-mutant (*csp-Δ*) shed cells for apoptotic characteristics, specifically phosphatidylserine exposure and TdT-mediated dUTP nick end labelling (TUNEL)-reactive DNA fragments. Like floaters that undergo caspase-mediated apoptosis

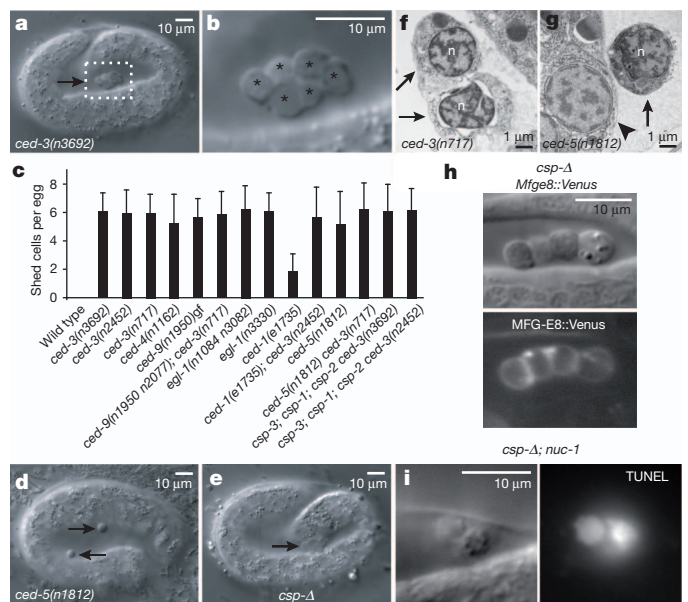


Figure 1 | Cells with apoptotic morphology are shed from *C. elegans* embryos lacking caspase activity. **a, b**, Low (**a**) and high (**b**) magnification differential interference contrast (DIC) images of a *ced-3(n3692)* egg with a cluster of six cells that detached from the embryo. Asterisks indicate individual shed cells in **b**. **c**, Quantification of shed cells or floaters in mutants defective in programmed cell death and/or corpse engulfment. Error bars denote s.d. **d**, A *ced-5(n1812)* egg with two floaters (indicated by arrows). **e**, A *csp-Δ* egg with a cluster of five shed cells (indicated by arrow). **f, g**, Transmission electron micrographs of shed cells from *ced-3(n717)* (**f**) and *ced-5(n1812)* (**g**) embryos. Arrows denote shed cells and arrowhead denotes an embryonic cell in **g**, n, nucleus. **h**, The phosphatidylserine binding protein MFG-E8 expressed from the transgene *nIs398[P_{dym-1}::Mfge8::Venus]* associates with the surface of *csp-Δ* shed cells. **i**, The shed cells of *csp-Δ; nuc-1(e1392)* eggs are TUNEL reactive.

¹Howard Hughes Medical Institute and Department of Biology, Massachusetts Institute of Technology, Cambridge, Massachusetts 02139, USA.

(Supplementary Fig. 2)⁸, the *msp-4* shed cells were reactive to the phosphatidylserine-binding protein MFG-E8 and to TUNEL staining (Fig. 1h, i). Also, *ced-3*-mutant shed cells showed chromatin condensation (darkly staining nuclear material) and separation of the nuclear envelope double membrane in transmission electron micrographs (Fig. 1f and Supplementary Fig. 3). These apoptotic features were present in *ced-5*-mutant floaters (Fig. 1g and Supplementary Fig. 3), although the cytoplasm of *ced-5*-mutant floaters were more compact. We conclude that the shed cells of embryos lacking caspase activity are in many respects cytologically and morphologically apoptotic, indicating that caspases are dispensable for many cellular changes that occur during apoptosis.

The somatic cell lineage of *C. elegans* is essentially invariant^{10,11}, allowing the precise identification of cell origins and fates. To determine the cellular identities of *ced-3*-mutant shed cells, we recorded time-lapse videos of developing *ced-3*-mutant embryos and traced the lineages of extruded cells in reverse (Fig. 2a, b and Supplementary Movie 1). We identified seven different cells eliminated by shedding from *ced-3*-mutant embryos (Fig. 2c), all of which are cells that normally die during wild-type embryogenesis. This finding is consistent with our observation that *ced-3*-mutant shed cells expressed *egl-1* (Fig. 2d), the transcription of which initiates programmed cell death¹², and with a previous report in which ABalpapaa (a cell fated to die) was observed detaching from a *ced-3*-mutant embryo⁵. The cells that can be shed are among the first to die in the wild-type embryo: 14 cells die within the first 300 min of development, and 7 of the 8 identified shed cells are among this group of 14 cells¹¹. Thus, specific cells fated to die early in embryogenesis can be eliminated by either canonical caspase-dependent apoptosis or by caspase-independent shedding.

To identify factors required for cell shedding, we tested genes involved in different cell-death processes and found that the generation of *ced-3*-mutant shed cells did not require genes that mediate germline apoptosis, cell-corpse engulfment, necrosis, autophagy or *lin-24*-mediated cell death (Supplementary Tables 1 and 3). We therefore developed a screening strategy based on the hypothesis that ABlpappap (one of the shed cells we identified; Fig. 2a, c) might

survive and adopt a fate associated with a lineally related cell in animals doubly defective in the canonical cell-death pathway and cell shedding. The sister cell of ABlpappap generates RMEV (a GABAergic (γ -aminobutyric acid-containing) neuron) and the excretory cell (Fig. 3a), which functions in osmoregulation¹³. We generated a *pig-12::cNLS::gfp* transgene to express green fluorescent protein (GFP) specifically in the excretory cell and observed that wild-type and *ced-3*-mutant animals contained a single GFP-positive cell (Fig. 3b, d). Using this reporter, we screened mutagenized *ced-3*-mutant animals and identified double mutants with a two-excretory-cell (Tex) phenotype. Two such Tex isolates, *n5433* and *n5437*, are alleles of the gene *pig-1* (*gm344A*) had one excretory cell (Fig. 3d), whereas 89% of *pig-1* (*gm344*) *ced-3* (*n3692*) double mutants contained two GFP-positive nuclei that resembled the large nucleus of the excretory cell (Fig. 3c, d and Supplementary Fig. 4). Double mutants with *pig-1* and *ced-4*, *ced-9* (gain-of-function) or *egl-1* mutations were similar to *pig-1* *ced-3* mutant animals (Supplementary Table 4). Inactivation of *pig-1* by RNA interference (RNAi) treatment phenocopied *gm344*, *n5433* and *n5437*, confirming that loss of *pig-1* function caused the Tex phenotype in these mutants (Supplementary Table 7).

The LIN-3 epidermal growth factor ligand is expressed embryonically by the excretory cell¹⁴, and *pig-1* *ced-3* mutant embryos contained an extra cell that expressed *lin-3* (Supplementary Fig. 5a). Furthermore, the heads of *pig-1* *ced-3* mutant animals contained large cysts (Fig. 3e) similar to those of mutants with defective excretory cell function¹³. Thus, *pig-1* *ced-3* mutants generated an ectopic excretory cell, albeit one that either was defective in osmoregulation or interfered with the function of the endogenous excretory cell.

To address whether the ectopic excretory cell of *pig-1* *ced-3* mutants is derived from the un-shed ABlpappap cell, we examined directly the fate of ABlpappap in *pig-1* and *pig-1* *ced-3* mutant embryos (Supplementary Movies 2 and 3). In *pig-1*-mutant embryos (and as in wild type), ABlpappap became a highly refractile cell corpse within 45 min of its generation (Fig. 3f; data not shown). By contrast, ABlpappap survived and divided approximately 115 min after it was generated in *pig-1* *ced-3* mutant embryos (Fig. 3g). In the three *pig-1* *ced-3* mutant embryos we examined, neither ABlpappap nor its descendants detached from the embryo, suggesting that an ABlpappap descendant gives rise to the ectopic excretory cell in *pig-1* *ced-3* mutant larvae. As reported previously¹⁵, *pig-1* *ced-3* animals also contain ectopic RME-like neurons (Supplementary Fig. 5b and Supplementary Table 5), suggesting that when ABlpappap survives it generates both an ectopic RME-like and an ectopic excretory-like cell.

pig-1 inactivation by mutation or RNAi treatment reduced the number of shed cells in *ced-3*-, *ced-4*- or *ced-9* (gain-of-function)-mutant embryos by nearly 75% ($P < 5.0 \times 10^{-7}$ for each pair-wise comparison, Student's *t*-test; Fig. 3h; data not shown), demonstrating that *pig-1* is generally required for the generation of shed cells. Given this observation, the effects of *pig-1* on cell shedding are in several ways comparable to the effects of *ced-3* on programmed cell death: (1) *ced-3* affects most programmed cell deaths and *pig-1* similarly affects most shed cells, indicating that *ced-3* and *pig-1* act generally to drive programmed cell death and generate shed cells, respectively; (2) like programmed cell deaths, extruded cells share morphologic and genetic properties and can be viewed as expressing a specific cell fate; and (3), like mutations in *ced-3*, mutations in *pig-1* cause cells that should die to express the fates of cells that normally survive.

pig-1 encodes a homologue of MELK, an AMPK-related serine-threonine kinase required cell autonomously for the asymmetric cell divisions of many *C. elegans* neuroblasts^{15,16}. Mammalian AMPK-related kinases control metabolism and cell polarity¹⁷ and are activated through phosphorylation of a conserved threonine within their T-loop domains by the kinase LKB1 (also known as STK11) (ref. 18) and its complex partners STRAD α and MO25 α (also known as CAB39) (refs 19, 20). The PIG-1 T-loop threonine (T169) was necessary for a

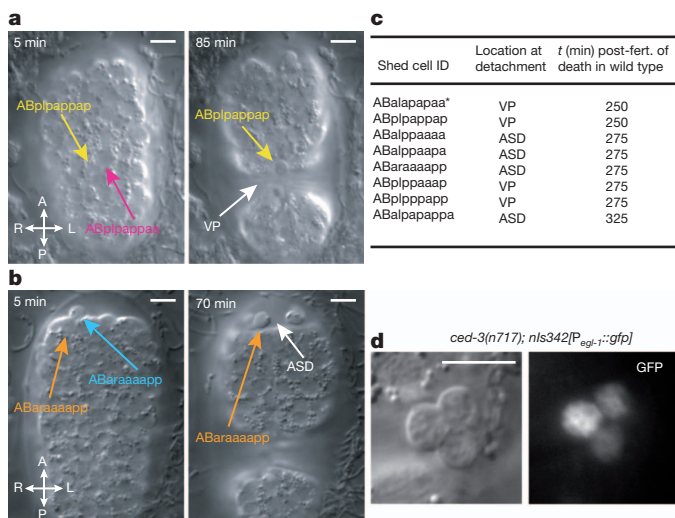


Figure 2 | Cells that are shed from *ced-3*-mutant embryos are normally fated to die early during wild-type embryogenesis. **a, b**, DIC micrographs of *ced-3* (*n3692*) embryos showing ABlpappap (**a**) and ABaraaaapp (**b**) 5 min after generation and shortly after shedding from the embryo (85 and 70 min later, respectively). ASD, anterior sensory depression; VP, ventral pocket. **c**, Cells that can be shed from *ced-3* (*n3692*) embryos, their locations when extruded and the timings of their deaths in wild-type embryos¹¹. Asterisk denotes data reported in ref. 5. **d**, DIC and fluorescence micrographs of shed cells from a *ced-3* (*n717*) embryo containing the *nIs342[P_{egl-1}::gfp]* transgene, which expresses GFP from the *egl-1* promoter. Scale bars, 10 μ m.

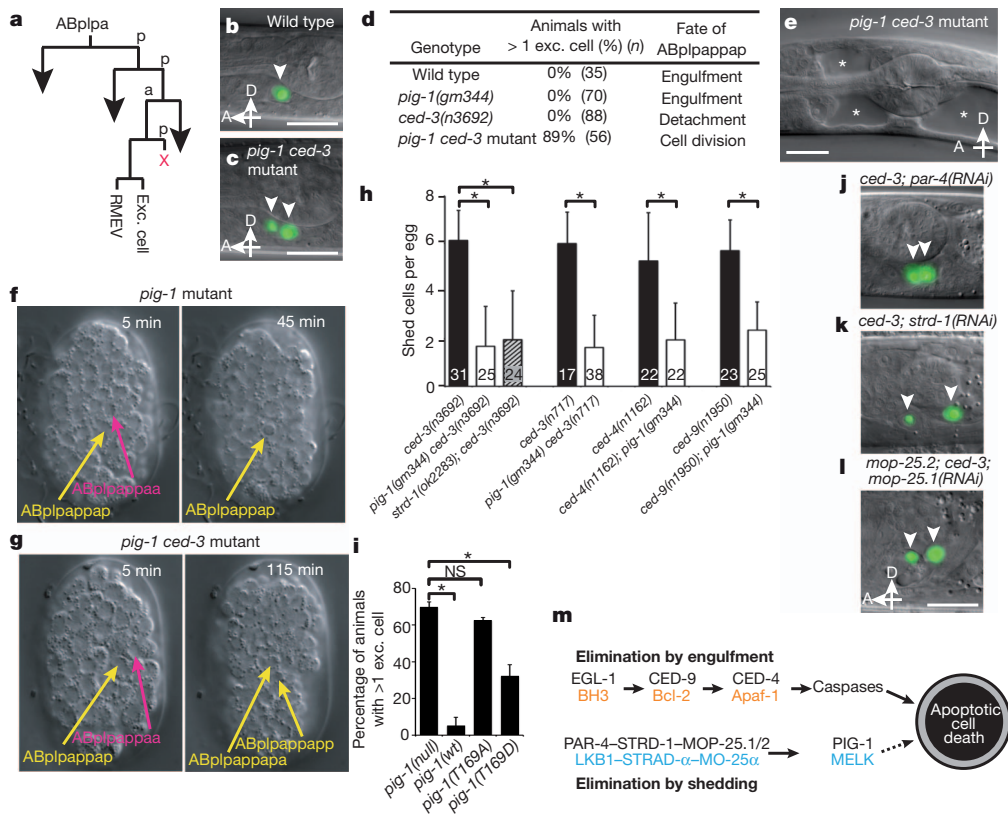


Figure 3 | The LKB1 homologue PAR-4 and the AMPK-related kinase PIG-1 are required for cell shedding from *ced-3* embryos. **a**, The sub-lineage that produces the shed cell ABpplpapp, which is the lineal aunt of the neuron RMEV and the excretory cell (exc. cell). **b, c**, Merged DIC and fluorescence micrographs of wild-type (**b**) and *pig-1(gm344) ced-3(n3692)* (**c**) larvae containing the transgene *nIs434[P_{pgp-12::gfp}]*, which expresses GFP in the excretory cell. Arrowheads indicate excretory and ectopic excretory-like cells. **d**, Percentage of L3 larvae with ectopic excretory cells. All genotypes contained *nIs434[P_{pgp-12::gfp}]*. **e**, The head of a larval *pig-1(gm344) ced-3(n3692)* animal containing large cysts (asterisks). **f, g**, The fate of the cell ABpplpapp in *pig-1(gm344)* and *pig-1(gm344) ced-3(n3692)* embryos. **f**, ABpplpapp in a *pig-1* mutant embryo shown 5 min after its generation and shortly after it underwent programmed cell death 45 min later. **g**, ABpplpapp in a *pig-1 ced-3* mutant embryo shown 5 min after its generation and immediately after it divided 115 min later. **h**, *pig-1* and *strd-1* are required for cell shedding. Mutation of *pig-1* and of *strd-1* reduced the number of shed cells in *ced-3*, *ced-4* or *ced-9* (gain-of-

pig-1 transgene to rescue the ectopic excretory cell defect of *pig-1 ced-3* mutants, whereas changing T169 to a phosphomimetic aspartic acid bypassed this requirement (Fig. 3i), indicating that PIG-1 is probably activated by phosphorylation of its T-loop. We therefore tested the *C. elegans* homologues of LKB1, STRAD and MO25 (*par-4*, *strd-1* and paralogues *mop-25.1*, *mop-25.2* and *mop-25.3*, respectively) for roles in the elimination of ABpplpapp. *par-4* or *strd-1* inactivation caused the Tex phenotype in *ced-3* mutants (Fig. 3j, k and Supplementary Table 6). Furthermore, the *ok2283* deletion allele of *strd-1* reduced the number of shed cells in *ced-3*-mutant embryos by 67% ($P = 1.9 \times 10^{-10}$, Student's *t*-test; Fig. 3h). The inactivation of both *mop-25.1* and *mop-25.2* was necessary to cause the Tex defect in *ced-3* mutants (Fig. 3l and Supplementary Table 6), indicating redundant function. We conclude that both PIG-1 and the PAR-4-STRD-1-MOP-25 complex are required for cell shedding in *C. elegans*.

Our genetic analyses suggest that PIG-1 and PAR-4 function in the same pathway. The deletion mutation *ok2283*, a putative null allele of *strd-1* (Supplementary Table 8), failed to enhance any of the *pig-1* or *pig-1 ced-3* defects (Fig. 4h, i and Supplementary Fig. 6 and Supplementary Tables 8 and 9). Although, *par-4* and *strd-1* can act independently²¹, this result suggests that PIG-1 and PAR-4 and its binding

function (gf) eggs. Error bars denote s.d. $P < 5 \times 10^{-7}$, Student's *t*-test. **i**, The T-loop threonine (T169) of PIG-1 is required for the elimination of ABpplpapp. Average percentage of larvae with ectopic excretory cells from multiple *pig-1(gm344) ced-3(n3692)* lines carrying the following *pig-1* transgenes: *pig-1(wt)*, the wild-type *pig-1* genomic locus (three lines, $n = 42, 47$ and 58); *pig-1(null)*, two STOP codons in the first exon (three lines, $n = 40, 43$ and 45); *pig-1(T169A)*, threonine 169 changed to alanine (three lines, $n = 40, 41$ and 48); and *pig-1(T169D)*, threonine 169 changed to aspartic acid (five lines, $n = 31, 32, 43, 48$ and 50). Error bars denote s.e.m. $P > 0.05$ (Student's *t*-test). NS, not significant ($P < 10^{-3}$). **j-l**, Merged DIC and fluorescence micrographs of *ced-3(n3692); par-4(RNAi)* (**j**), *ced-3(n3692); strd-1(RNAi)* (**k**), and *mop-25.2(ok2073); ced-3(n3692); mop-25.1(RNAi)* (**l**) larvae carrying *nIs434[P_{pgp-12::gfp}]*. Arrowheads indicate excretory and ectopic excretory-like cells. **m**, Redundant pathways mediate the elimination of ABpplpapp and other cells shed from *ced-3*-mutant embryos. Mammalian counterparts of proteins involved in cell elimination are shown in orange and blue. Scale bars, 10 μ m.

partners function in the same pathway. We believe that PIG-1 is the phosphorylation target of PAR-4 in cell shedding because inactivation of PIG-1 but of no other AMPK-related kinase caused the survival of ABpplpapp in *ced-3* mutants (Supplementary Table 7). The Tex defect of *pig-1(gm344) ced-3(n3692)* animals (89%) was higher than that of *strd-1(ok2283); ced-3(n3692)* animals (43%) (Fig. 3d and Supplementary Table 4). Thus, STRD-1 and possibly the entire PAR-4 complex are required partially for PIG-1 activation, indicating that other factors, or PIG-1 itself through autophosphorylation, also stimulate PIG-1 activity. Indeed, MELK phosphorylates itself *in vitro*¹⁸.

To investigate how PIG-1 regulates cell shedding, we reasoned that shed cells must be deficient in adhesive contacts with the embryo and explored whether *pig-1* modulates cell-adhesion complexes, specifically adherens junctions. In *C. elegans*, adherens junctions comprise a cadherin-catenin complex and a complex including DLG-1 (a homologue of the *Drosophila* discs large protein) and AJM-1. Both complexes participate in the enclosure of the embryo within a layer of epidermal cells²², a major morphogenic event that coincides with the detachment of shed cells.

We examined the expression of AJM-1, DLG-1, HMP-1 (α -catenin) and JAC-1 (p120 catenin) fused to GFP in shed cells. AJM-1, DLG-1

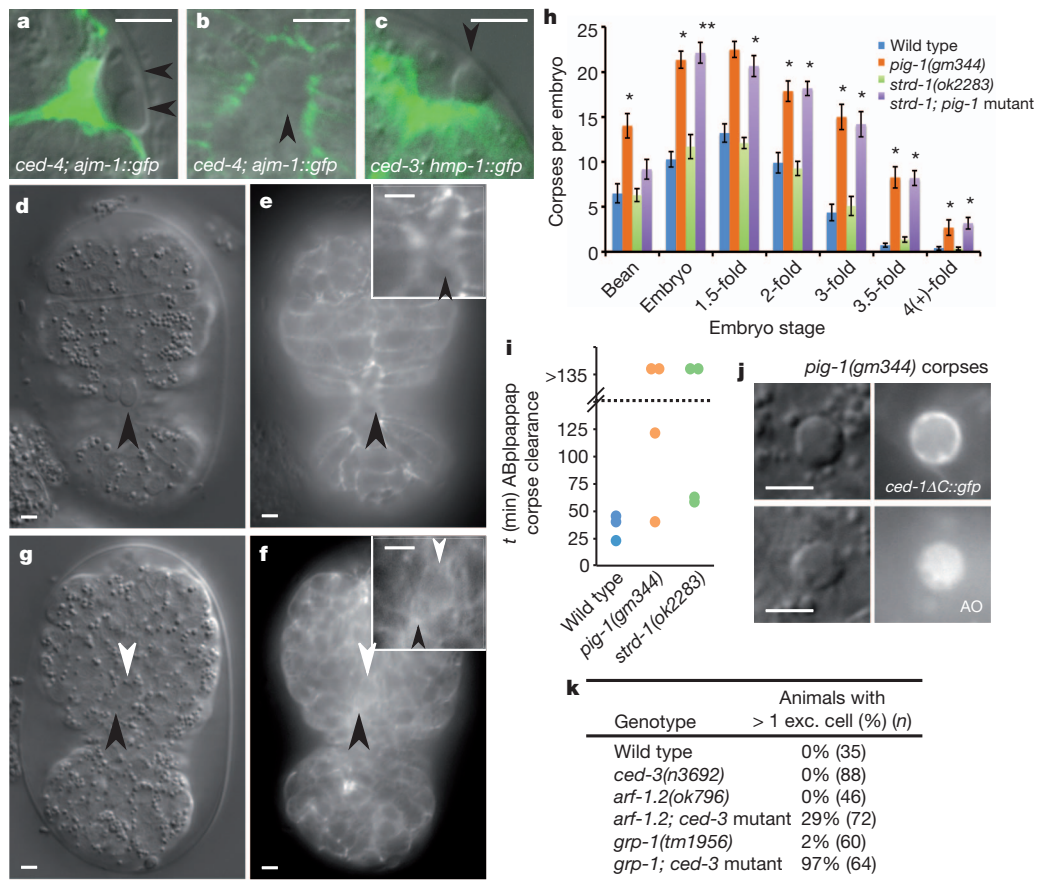


Figure 4 | Shed cells lack cell-adhesion molecules that are inappropriately expressed in *pig-1* mutants, possibly because of impaired endocytosis.

a–c, Merged DIC and confocal fluorescence micrographs of shed cells from *ced-4(n1162); jcls1[ajm-1::gfp]* (**a**, **b**) and *ced-3(n3692); jcls17[hmp-1::gfp]* (**c**) eggs. Arrowheads indicate detached shed cells. **d–g** DIC and epifluorescence micrographs of *ced-3(n3692); jcls17[hmp-1::gfp]* (**d**, **e**) and *pig-1(gm344) ced-3(n3692); jcls17[hmp-1::gfp]* (**f**, **g**) embryos just before the completion of ventral enclosure. Black arrowheads indicate ABplpappap (**d**, **e**) or its descendant (**f**, **g**); white arrowheads indicate excretory cell (ABplpappap). Insets, magnification of ABplpappap or the excretory cell and the ABplpappap

and HMP-1 were not visible at the surface of *ced-3*- or *ced-4*-mutant shed cells that had recently detached from either the anterior sensory depression (Fig. 4a, c and Supplementary Fig. 7b) or the ventral cleft (Fig. 4b and Supplementary Fig. 7a) (JAC-1::GFP was detectable in some shed cells; Supplementary Fig. 7c). The absence of cell-adhesion proteins was noteworthy given their presence on adjacent epidermal cells (Fig. 4a–c and Supplementary Fig. 7). ABplpappap in *ced-3*-mutant embryos remained at the ventral surface of the embryo from its generation until its detachment and never expressed HMP-1::GFP (Fig. 4d, e; data not shown). By contrast, in *pig-1 ced-3* mutant embryos, ABplpappap ingress dorsally during ventral enclosure (Fig. 4f), matching the movement of the excretory cell away from the ventral surface¹⁴. Notably, ABplpappap and its descendants exhibited a uniform expression of HMP-1::GFP at the cell surface (Fig. 4g), indicating that a loss of *pig-1* function results in the inappropriate expression of cell-adhesion molecules. Thus, PIG-1 might facilitate cell shedding by preventing the expression of cell-adhesion molecules on the surfaces of shed cells.

Several lines of evidence suggest that *pig-1* promotes shed-cell detachment through endocytosis. Many cell corpses, including the ABplpappap corpse, were not cleared efficiently in *pig-1*-mutant embryos (Fig. 4h, i). The *pig-1*-mutant cell corpses were encircled rapidly by the engulfment receptor CED-1 and stained positively with acridine orange, a marker of internalized corpses (Fig. 4j and

descendant in **f**, **g**, **h**). Number of persistent cell corpses in wild-type, *pig-1(gm344)*, *strd-1(ok2283)* and *strd-1(ok2283); pig-1(gm344)* embryos. *n* values are provided in Supplementary Table 11. Error bars denote s.e.m. $P < 0.002$ for pair-wise comparison with wild type (Student's *t*-test). **i**, Time required for engulfment and degradation of ABplpappap cell corpses in wild-type, *pig-1(gm344)* or *strd-1(ok2283)* embryos. **j**, DIC and fluorescence micrographs of cell corpses from 'bean'-stage *pig-1(gm344)* embryos carrying either the *nIs400[P_{ced-1}::ced-1ΔC::gfp]* transgene or stained with acridine orange (AO). **k**, Percentage of L3 larvae with ectopic excretory cells. All genotypes contained *nIs434[P_{pgp-12}::gfp]*. Scale bars, 5 μm.

Supplementary Fig. 8). These results demonstrate that the delay in clearance was after engulfment and reflected a defect in corpse degradation, a process that requires endocytic pathway components²³. Interestingly, a recent study showed that two *C. elegans* ARF GTPase genes, *arf-1.2* and *arf-6*, and a gene coding for an ARF GTPase-activating protein, *cnt-2*, have functions in cell-fate determination similar to those of *pig-1* as well as roles in receptor-mediated endocytosis²⁴. Mammalian ARF GTPases function in endocytosis²⁵ and can remove cadherin complexes from the cell surface²⁶. We noted that inactivation of ARF GTPase genes *arf-1.2* or *arf-3* or the ARF guanine exchange factor gene *grp-1* also produced ectopic excretory cells in *ced-3* mutants (Fig. 4k and Supplementary Table 10).

Taken together, our observations suggest that the PAR-4 complex, PIG-1 and ARF GTPases promote the detachment of shed cells through the endocytosis-mediated removal of cell-adhesion molecules from the cell surface. Thus, the programmed elimination and apoptosis of at least eight *C. elegans* cells can be accomplished through either canonical caspase-mediated apoptosis involving the engulfment of dying cells or a caspase-independent shedding mechanism that also results in apoptosis and that requires the PAR-4 complex and the AMPK-related kinase PIG-1 (Fig. 3m). These two mechanisms are functionally redundant, as ABplpappap and the other shed cells survive only in mutants in which both pathways are disrupted.

We propose that cell shedding is an evolutionarily conserved mechanism of cell elimination. Many epithelia extrude cells constitutively to maintain tissue homeostasis, and the shed epithelial cells of vertebrates share features with the shed cells of caspase-deficient *C. elegans* embryos. First, like other shed epithelial cells⁴, shed intestinal enterocytes frequently show apoptotic markers^{27,28}, including caspase-3 activation and TUNEL reactivity. Second, despite the apoptotic appearance of shed enterocytes, the intestinal epithelia of *Casp3*^{-/-}, *Apaf1*^{-/-}, *Bax*^{-/-}, *Bak1*^{-/-} or *Bcl2*-overexpressing mice are not grossly abnormal^{2,29}, suggesting that cell extrusion is not dependent on caspase-mediated cell killing. Third, *LKB1* mutations cause Peutz–Jeghers syndrome³⁰, which is characterized by intestinal hamartomas (polyps) containing excess epithelial cells. It is possible that *LKB1* mutations contribute to polyp formation by causing a defect in the extrusion of epithelial cells. On the basis of our observations of *C. elegans*, we predict that the PIG-1 homologue MELK could be a target of *LKB1* in the gastrointestinal tract and that mutations of *MELK* might also impair enterocyte shedding and cause a polyposis phenotype in the mammalian intestine.

METHODS SUMMARY

DIC and epifluorescence micrographs were obtained using an Axioskop II (Zeiss) compound microscope, an ORCA-ER CCD camera (Hamamatsu) and OpenLab software (Agilent) and modified using ImageJ software (National Institutes of Health). For the time-lapse experiments, early (two- or four-cell stage) embryos were dissected from gravid adults, mounted on a slide with a 4% agar pad and covered with a cover slip sealed to the slide with petroleum jelly to prevent the preparation from drying. The developing embryos were imaged every 4 min for a total of 300 min, and at each time point a Z-stack of 50 images spaced at 0.6 μm was acquired. Confocal microscopy was performed using a Zeiss LSM 510 instrument, and the resulting images were modified using ImageJ software. Shed cells or floaters were counted in eggs between the 2-fold and 3.5-fold stages of development (approximately 450–600 min after the first cell division) using a ×100 objective equipped with DIC optics. The numbers of excretory cells and excretory-like cells were counted in L3 larvae carrying the *P_{gpp-12::gfp}* transcriptional reporter using a ×100 objective. A cell was scored as being ‘excretory-cell-like’ if it was located in the anterior third of the animal and its nucleus strongly expressed GFP.

Full Methods and any associated references are available in the online version of the paper.

Received 4 April 2011; accepted 17 May 2012.

Published online 15 July 2012.

- Fuchs, Y. & Steller, H. Programmed cell death in animal development and disease. *Cell* **147**, 742–758 (2011).
- Reddien, P. W. & Horvitz, H. R. The engulfment process of programmed cell death in *Caenorhabditis elegans*. *Annu. Rev. Cell Dev. Biol.* **20**, 193–221 (2004).
- Yuan, J. & Kroemer, G. Alternative cell death mechanisms in development and beyond. *Genes Dev.* **24**, 2592–2602 (2010).
- Rosenblatt, J., Raff, M. C. & Cramer, L. P. An epithelial cell destined for apoptosis signals its neighbors to extrude it by an actin- and myosin-dependent mechanism. *Curr. Biol.* **11**, 1847–1857 (2001).
- Ellis, H. M. & Horvitz, H. R. Genetic control of programmed cell death in the nematode *C. elegans*. *Cell* **44**, 817–829 (1986).
- Abraham, M. C., Lu, Y. & Shaham, S. A morphologically conserved nonapoptotic program promotes linker cell death in *Caenorhabditis elegans*. *Dev. Cell* **12**, 73–86 (2007).
- Shaham, S., Reddien, P. W., Davies, B. & Horvitz, H. R. Mutational analysis of the *Caenorhabditis elegans* cell-death gene *ced-3*. *Genetics* **153**, 1655–1671 (1999).
- Wu, Y. C., Stanfield, G. M. & Horvitz, H. R. NUC-1, a *Caenorhabditis elegans* DNase II homologue, functions in an intermediate step of DNA degradation during apoptosis. *Genes Dev.* **14**, 536–548 (2000).

- Shaham, S. Identification of multiple *Caenorhabditis elegans* caspases and their potential roles in proteolytic cascades. *J. Biol. Chem.* **273**, 35109–35117 (1998).
- Sulston, J. E. & Horvitz, H. R. Post-embryonic cell lineages of the nematode, *Caenorhabditis elegans*. *Dev. Biol.* **56**, 110–156 (1977).
- Sulston, J. E., Schierenberg, E., White, J. G. & Thomson, J. N. The embryonic cell lineage of the nematode *Caenorhabditis elegans*. *Dev. Biol.* **100**, 64–119 (1983).
- Potts, M. B. & Cameron, S. Cell lineage and cell death: *Caenorhabditis elegans* and cancer research. *Nature Rev. Cancer* **11**, 50–58 (2011).
- Buechner, M. Tubes and the single *C. elegans* excretory cell. *Trends Cell Biol.* **12**, 479–484 (2002).
- Abdus-Saboor, I. et al. Notch and Ras promote sequential steps of excretory tube development in *C. elegans*. *Development* **138**, 3545–3555 (2011).
- Cordes, S., Frank, C. A. & Garriga, G. The *C. elegans* MELK ortholog PIG-1 regulates cell size asymmetry and daughter cell fate in asymmetric neuroblast divisions. *Development* **133**, 2747–2756 (2006).
- Ou, G., Stuurman, N., D'Ambrosio, M. & Vale, R. D. Polarized myosin produces unequal-size daughters during asymmetric cell division. *Science* **330**, 677–680 (2010).
- Shackelford, D. B. & Shaw, R. J. The *LKB1*–AMPK pathway: metabolism and growth control in tumour suppression. *Nature Rev. Cancer* **9**, 563–575 (2009).
- Lizcano, J. M. et al. *LKB1* is a master kinase that activates 13 kinases of the AMPK subfamily, including MARK/PAR-1. *EMBO J.* **23**, 833–843 (2004).
- Boudeau, J. et al. MO25^{α/β} interact with STRAD^{α/β} enhancing their ability to bind, activate and localize *LKB1* in the cytoplasm. *EMBO J.* **22**, 5102–5114 (2003).
- Zeqiraj, E., Filippi, B. M., Deak, M., Alessi, D. R. & van Aalten, D. M. F. Structure of the *LKB1*–STRAD–MO25 complex reveals an allosteric mechanism of kinase activation. *Science* **326**, 1707–1711 (2009).
- Narbonne, P., Hyenne, V., Li, S., Labbé, J.-C. & Roy, R. Differential requirements for STRAD in *LKB1*-dependent functions in *C. elegans*. *Development* **137**, 661–670 (2010).
- Labouesse, M. Epithelial junctions and attachments. *WormBook* **13**, 1–21 (2006).
- Kinchen, J. M. et al. A pathway for phagosome maturation during engulfment of apoptotic cells. *Nature Cell Biol.* **10**, 556–566 (2008).
- Singhvi, A. et al. The Arf GAP CNT-2 regulates the apoptotic fate in *C. elegans* asymmetric neuroblast divisions. *Curr. Biol.* **21**, 948–954 (2011).
- D'Souza-Schorey, C. & Chavrier, P. ARF proteins: roles in membrane traffic and beyond. *Nature Rev. Mol. Cell Biol.* **7**, 347–358 (2006).
- D'Souza-Schorey, C. Disassembling adherens junctions: breaking up is hard to do. *Trends Cell Biol.* **15**, 19–26 (2005).
- Potten, C. S. Stem cells in gastrointestinal epithelium: numbers, characteristics and death. *Phil. Trans. R. Soc. Lond. B* **353**, 821–830 (1998).
- Watson, A. J. M., Duckworth, C. A., Guan, Y. & Montrose, M. H. Mechanisms of epithelial cell shedding in the mammalian intestine and maintenance of barrier function. *Ann. NY Acad. Sci.* **1165**, 135–142 (2009).
- Coopersmith, C. M., O'Donnell, D. & Gordon, J. I. *Bcl-2* inhibits ischemia-reperfusion-induced apoptosis in the intestinal epithelium of transgenic mice. *Am. J. Physiol.* **276**, G677–G686 (1999).
- Hemminki, A. et al. A serine/threonine kinase gene defective in Peutz–Jeghers syndrome. *Nature* **391**, 184–187 (1998).

Supplementary Information is linked to the online version of the paper at www.nature.com/nature.

Acknowledgements We thank Z. Zhou, T. Hirose and S. Nakano for reporter constructs; B. Castor, E. Murphy and R. Droste for determining DNA sequences; S. Dennis for screening of the deletion library; N. An for strain management; and, J. Yuan, S. Nakano, N. Paquin, C. Engert and A. Saffer for discussions. The *Caenorhabditis* Genetic Center, which is funded by the National Institutes of Health National Center for Research Resources (NCR), provided many strains. S. Mitani provided *gpp-1(tm1956)*. D.P.D. was supported by post-doctoral fellowships from the Damon Runyon Cancer Research Foundation and from the Charles A. King Trust. H.R.H. is the David H. Koch Professor of Biology at the Massachusetts Institute of Technology and an Investigator at the Howard Hughes Medical Institute.

Author Contributions D.P.D. and H.R.H. designed the experiments, analysed the data and wrote the manuscript. D.P.D. and V.H. performed the experiments.

Author Information Reprints and permissions information is available at www.nature.com/reprints. The authors declare no competing financial interests. Readers are welcome to comment on the online version of this article at www.nature.com/nature. Correspondence and requests for materials should be addressed to H.R.H. (horvitz@mit.edu).

METHODS

Strains. All *C. elegans* strains were cultured as described previously³¹ and maintained at 20 °C unless noted otherwise. We used the Bristol strain N2 as the wild-type strain. The mutations used in our experiments were as follows: LGI: *ced-1(e1735)*, *cep-1(gk138)*, *esp-3(n4872)*, *dapk-1(gk219)*, *gpb-2(ad541)*, *lin-35(n745)*, *nIs433[P_{pgp-12::gfp}, unc-76(+)]*; LGII: *cad-1(j1)*, *esp-1(n4967)*, *mop-25.2(ok2073)*; LGIII: *arf-1.2(ok796)*, *ced-4(n1162)*, *ced-6(n1813)*, *ced-7(n1892)*, *ced-9(n1950)*, *n1950 n2077*, *ced-12(n3261)*, *grp-1(tm1956)*, *strd-1(ok2283)*, *nIs400[P_{ced-1::ced-1ΔC::gfp}, P_{myo-2::dsRed}]*; LGIV: *ced-2(e1752)*, *ced-3(n717)*, *n2452*, *n3692*, *ced-5(n1812)*, *ced-10(n1993)*, *esp-2(n4871)*, *ham-1(n1438)*, *lin-24(n4294)*, *lin-33(n4514)*, *pig-1(gm344)*, *n5433*, *n5437*, *jcls1[ajm-1::gfp, rol-6(su1006)]*; LGV: *unc-76(e911)*, *par-4(it57)*, *egl-1(n1084)*, *n3082*, *n3330*, *crt-1(ok948)*, *unc-68(e540)*, *unc-51(e369)*, *nIs342[P_{egl-1::gfp}, lin-15(+)]*; LGX: *nuc-1(e1392)*, *lin-15A(n765)*, *nIs434[P_{pgp-12::gfp}, unc-76(+)]*; unknown linkage: *nIs398[P_{dym-1::mfge8::Venus}, P_{myo-2::dsRed}]*, *jcls17[hmp-1::gfp, dlgl-1::dsRed, rol-6(su1006)]*, *nIs201[P_{unc-25::4xNLS::mStrawberry}, plin-15EK]*, *xnIs17[dlgl-1::gfp, rol-6(su1006)]*, *syIs107[lin-3::gfp]*, *jcls25[P_{hmr-1::jac-1::gfp::unc-54(3' UTR)}, rol-6(su1006)]*; extrachromosomal arrays: *nEx1747*, *nEx1748* and *nEx1749* [*pig-1(wt)*], *P_{pgp-12::gfp}*, *P_{myo-2::dsRed}]*; *nEx1758*, *nEx1759* and *nEx1760* [*pig-1(STOP)*], *P_{pgp-12::gfp}*, *P_{myo-2::dsRed}]*; *nEx1755*, *nEx1756* and *nEx1757* [*pig-1(T169A)*], *P_{pgp-12::gfp}*, *P_{myo-2::dsRed}]*; *nEx1831*, *nEx1832*, *nEx1833*, and *nEx1834* [*pig-1(T169D)*], *P_{pgp-12::gfp}*, *P_{myo-2::dsRed}]*.

Plasmids. The *P_{egl-1::gfp}* transcriptional reporter and the *P_{dym-1::Mfge8::Venus}* (pV559) translation reporter have been described previously^{32,33}. The *P_{unc-25::mStrawberry}* transcriptional reporter (pSN223) was constructed using PCR to amplify a 1.8 kb fragment of the *unc-25* promoter region with the primers 5'-CGAATTTTTCGATGCAAAAACACCCACTTTTTCGATC-3' and 5'-CGG GATCCTCGAGCACAGCATCATCTTCGTCAGCAGC-3'. The resulting amplicon was digested with SphI and BamHI and ligated into pSN199, which encodes the 4xNLS::mStrawberry fusion. pSN199 was constructed by replacing the AgeI-EcoRI fragment of pPD122.56 with the AgeI-EcoRI fragment from the plasmid mStrawberry 6. The transcriptional reporter *P_{pgp-12::gfp}* (pSN359) was constructed using PCR to amplify a 2.9 kb fragment of the *pgp-12* promoter region with the primers 5'-GCAAGCTTGTGCTTTCAGTGAACAGAAACT-3' and 5'-CCTC TAGAATTCATCAATTGGCTCGATCGCA-3'. The resulting amplicon was digested with HindIII and XbaI and ligated into pPD122.56. The *pig-1*-rescuing construct (pDD078) was constructed using PCR to amplify three overlapping genomic fragments spanning 17.5 kb with the following primer pairs: 5'-CAG TGAGCGCGTAATACGACTACTATAGGGCGAATTGGCCACATCAAA TGAAAGACG-3' and 5'-TCAGAGTTCAATATATGTTGG-3'; 5'-TGTCT ACACCCTCCAAACACC-3' and 5'-ACGACGGCATCAGATATTCG-3'; and 5'-CCAAGCGCGCAATTAACCCTCAATAAGGGAACAAAAGCTTG ATGATGATGTCCTGAGC-3' and 5'-CATGTCCAACAATGGAATCG-3'. The resulting amplicons were ligated into pRS426 by homologous recombination in *Saccharomyces cerevisiae* (yeast-mediated ligation). The *pig-1(STOP)* (pDD084), *pig-1(T169A)* (pDD085) and *pig-1(T169D)* (pDD088) constructs were also generated by yeast-mediated ligation using a SfoI-NaeI-digested fragment of pDD078. *pig-1(STOP)* changes codons 8 and 9 to the stop codons TAG and TGA, respectively. *pig-1(T169A)* changes the T-loop threonine codon at position 169 to GCG, which encodes an alanine residue. *pig-1(T169D)* changes the T-loop threonine codon at position 169 to GAC, which encodes an aspartic acid residue. pDD073 (pL4440:*par-4*) was constructed using PCR to amplify the *par-4* complementary DNA with the following primers: 5'-GCGCGCGGATGG ATGCTCCGTCGACATCC-3' and 5'-GCGTCTAGACTAAGCATCATCGG TACGAG-3'. The resulting amplicon was digested with SacII and XbaI and then ligated into pL4440.

Shed cell, excretory cell, persistent corpse and extra pharyngeal cell counts. Shed cells or floaters were counted in eggs between the 2-fold and 3.5-fold stages of development (approximately 450–600 min after the first cell division) using a ×100 objective equipped with Nomarski differential interference contrast (DIC) optics. The number of excretory and excretory-like cells were counted in L3 larvae carrying the *P_{pgp-12::gfp}* transcriptional reporter using a ×100 objective. A cell was scored as an excretory cell if it was located in the anterior third of the animal and its

nucleus strongly expressed GFP. Persistent cell corpse and extra pharyngeal cell counts were performed as described previously³⁴.

Mutagenesis screen for synthetic *Tex* mutants. *ced-3(n3692)*; *nIs434* or *nIs433*; *ced-3(n3692)* L4 larvae were mutagenized with ethyl methanesulfonate as described previously³¹. Using a dissecting microscope equipped for the detection of GFP fluorescence, we screened approximately 25,000 F3 progeny of the mutagenized animals for an extra GFP+ cell near the posterior bulb of the pharynx. We showed by complementation testing and DNA sequence determination that two of the mutants isolated from this screen, *n5433* and *n5437*, were alleles of *pig-1*.

RNAi treatments. RNAi treatments were performed by feeding using RNAi constructs and reagents described previously^{35,36}. In brief, HT115 *Escherichia coli* carrying RNAi clones in the pL4440 vector were cultured overnight in Luria broth (LB) liquid media with antibiotics. Nematode growth media (NGM) plates containing 1 mM IPTG and antibiotics were seeded with the LB culture and incubated 24 h at 20 °C. Five L2 larvae were placed onto each seeded NGM plate, and the progeny of these animals were scored for either shed cells or ectopic excretory cells as described above. Control RNAi treatments were performed with the empty vector pL4440. The complete sequences of all RNAi sequences used in this study are provided in the Supplementary Information.

TUNEL and acridine orange staining. TUNEL reactions were performed as described previously^{8,37}. Fixation times (between 12 and 16 min) were optimized for labelling the floaters in *ced-5(n1812)*; *nuc-1(e1392)* eggs. *nuc-1(e1392)* facilitates the observation of TUNEL reactivity. Acridine orange staining of embryos was performed as described previously³⁸.

Transmission electron microscopy. Gravid *sem-4(n1378)*; *ced-5(n1812)* or *sem-4(n1971)*; *ced-3(n717)* adult animals were fixed by high-pressure freezing in an HPM10 high-pressure freezer by Abra. They were then substituted using an RMC FS-7500 freeze substitution system with 2% osmium, 2% water in acetone at −90 °C for 5 days, warmed to −20 °C over 14 h and then held at −20 °C for 16 h before warming to 0 °C. Samples were washed 6 × 20 min, infiltrated stepwise into Eponate 12 resin (Ted Pella) and polymerized at 60 °C. The resulting blocks were sectioned at 50 nm, post-stained with uranyl acetate and lead, and imaged with a JEM-1200EX II microscope (Jeol) using an AMT XR41 CCD camera. *sem-4* mutations cause eggs to accumulate in the hermaphrodite gonad, allowing more embryos (including more later stage embryos) to be analysed per sample.

Microscopy. Nomarski DIC and epifluorescence micrographs were obtained using an Axioskop II (Zeiss) compound microscope and OpenLab software (Agilent). Merged DIC and epifluorescence images were generated using ImageJ software (National Institutes of Health). For the time-lapse experiments, early (two- or four-cell stage) embryos were dissected from gravid adults, mounted on a slide with a 4% agar pad and covered with a cover slip that was sealed to the slide with petroleum jelly to prevent the preparation from drying. The developing embryos were imaged every 4 min for a total of 300 min, and at each time point a Z-stack of 50 images spaced at 0.6 μm was acquired. Confocal microscopy was performed using a Zeiss LSM 510 instrument, and the resulting images were prepared and modified using ImageJ software.

- Brenner, S. The genetics of *Caenorhabditis elegans*. *Genetics* **77**, 71–94 (1974).
- Hirose, T., Galvin, B. D. & Horvitz, H. R. Six and *Eya* promote apoptosis through direct transcriptional activation of the proapoptotic BH3-only gene *egl-1* in *Caenorhabditis elegans*. *Proc. Natl Acad. Sci. USA* **107**, 15479–15484 (2010).
- Venegas, V. & Zhou, Z. Two alternative mechanisms that regulate the presentation of apoptotic cell engulfment signal in *Caenorhabditis elegans*. *Mol. Biol. Cell* **18**, 3180–3192 (2007).
- Schwartz, H. T. A protocol describing pharynx counts and a review of other assays of apoptotic cell death in the nematode worm *Caenorhabditis elegans*. *Nature Protocols* **2**, 705–714 (2007).
- Fraser, A. G. et al. Functional genomic analysis of *C. elegans* chromosome I by systematic RNA interference. *Nature* **408**, 325–330 (2000).
- Rual, J. F. et al. Toward improving *Caenorhabditis elegans* phenome mapping with an ORFeome-based RNAi library. *Genome Res.* **14**, 2162–2168 (2004).
- Parrish, J. Z. & Xue, D. Functional genomic analysis of apoptotic DNA degradation in *C. elegans*. *Mol. Cell* **11**, 987–996 (2003).
- Lu, Q. et al. *C. elegans* Rab GTPase 2 is required for the degradation of apoptotic cells. *Development* **135**, 1069–1080 (2008).